Supporting Information

Strategy for the improvement of electrical conductivity of a 3D Zn(II)-coordination polymer doubly bridging by mesaconato and pyridyl-isonicotinoyl hydrazide Schottky diode device

Manik Shit,[a,†]Arnab Kanti Karan,[b]Dipankar Sahoo,[b]Nabin Baran Manik,[b] Basudeb Dutta*[a,c]and Chittaranjan Sinha*[a]

[a]Department of Chemistry, Jadavpur University, Jadavpur, Kolkata 700 032, India.E-mail: crsjuchem@gmail.com.

[b]Department of Physics, Condensed Matter Physics Research Centre, Jadavpur University, Kolkata 700032, India.

[c]Department of Chemical Sciences, Indian Institute of Science Education and Research Kolkata, Mohanpur, West Bengal 741246, India.

[†]Present Address: Narajole Raj College, Paschim Medinipur, Narajole - 721211, India.

Materials and general method

All the chemicals used during this work were purchased in reagent grade and were used without further purification. Infrared (IR) spectrum was recorded using a Perkin Elmer SPECTRUM II LITA FT-IR spectrometer. On the compound **1**, a PerkinElmer 240C elemental analyzer was used to conduct an elemental analysis (carbon, hydrogen, and nitrogen).Thermogravimetric analysis (TGA) was carried out using a Perkin Elmer Pyris Diamond TG/DTA thermal analyzer in a nitrogen atmosphere (flow rate: 50 cm^3 min^{-1}) at a temperature range of 30-800 °C with a heating rate of 10 °C/min. Powder X-ray diffraction measurements were made using a Bruker D8 Discover instrument (Cu-Kα source).We recorded UV/vis spectra using a PerkinElmer Lambda 25 spectrophotometer.

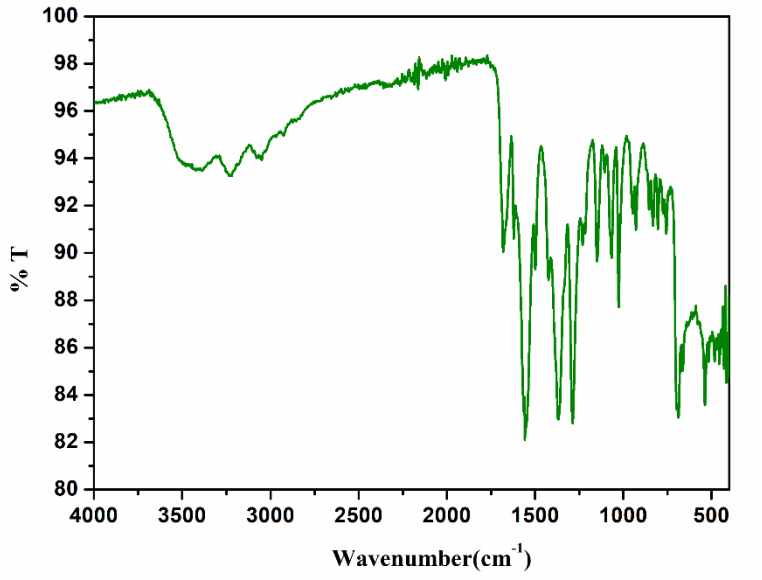

Figure S1. IR spectroscopy of Compound **1**.

DFT computation

Optimization of the gas phase geometry of the compound **1** was carried out using Density Functional Theory (DFT) calculation of Gaussian Program Package 09[1-3].All calculations were performed using SCXRD coordinates and B3LYP method. LanL2DZ basis set were employed for all elements including Zn. Different electronic transitions were theoretically determined using the time-dependent density functional theory (TDDFT) formalism calculation[4]. Vibrational frequency calculations were performed to ensure that the DFT-optimized geometries represent the local minima and only positive eigenvalues.

General X-ray Crystallography

A rod-shaped yellow colored single crystal of the compound **1** was taken for Single X-Ray Diffraction data collection using a Bruker SMART APEX-III CCD diffractometer furnished with graphite-monochromatic Mo-Kα radiation (λ=0.71073 Å). The structure of the compound was solved with direct method and was refined by full-matrix least squares on F2 using the SHELXL-2016/6[5]program package. The non-hydrogen atoms present in the architecture were well-refined with an isotropic thermal parameter. The hydrogen atoms were positioned in their geometrically idealized positions and controlled to ride on their parent atoms. Least squares refinements of all reflections within the hkl range $-13 \leq h \leq 13$, $-18 \leq k \leq 18$, $-17 \leq l \leq 17$ were utilized to carry out the unit cell parameters and crystal-orientation matrices. Collected data ($I>2\sigma(I)$) of crystal was integrated by employing the SAINT program[6]and the absorption correction was performed through SADABS[7].

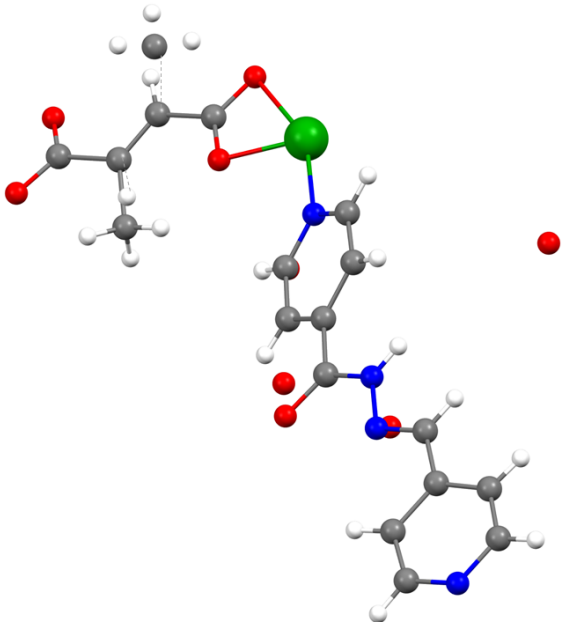

Figure S2. View of asymmetric unit along crystallographic axis b**.**

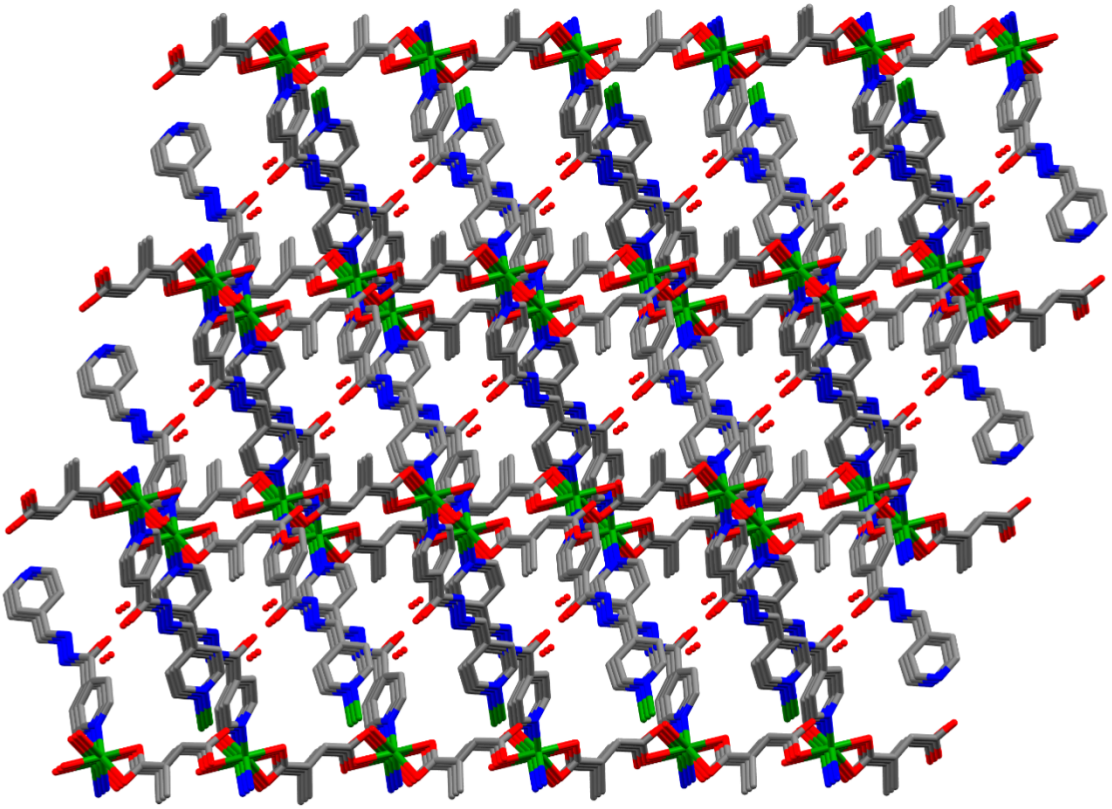

Figure S3. 3D structure of **1.**

Topology studies:

The analysis was performed with the topcryst.com[8]. The RCSR three-letter codes[9] were used to designate the network topologies. Those nets, that are absent in the RCSR, are designated with the TOPOS NDn nomenclature[10], where N is a sequence of coordination numbers of all non-equivalent nodes of the net, D is periodicity of the net (D=M, C, L, T for 0-,1-,2-,3-periodic nets), and n is the ordinal number of the net in the set of all non-isomorphic nets with the given ND sequence. To calculate the underlying nets, we used algorithms[11], the application of which for specific structures is discussed in the article[12]. The TTD collection was used to determine the topological type of the crystal structure.

Hirshfeld surface (HS) analysis

Hirshfeld surface and 2D finger print plot[13-16] were calculated with the help of CRYSTAL EXPLORER 3.1[17] using Crystal structure (CIF) file. The Hirshfeld surface was plotted over normalized contact distance (d_{norm})[18]. Shape index and decomposed fingerprint plot were presented in term of d_e vs d_i. The d_{norm}, expressed as

$$d_{norm} = (d_i - r_i^{vdw}) / r_i^{vdw} + (d_e - r_e^{vdw}) / r_e^{vdw}$$

where r_i^{vdw} and r_e^{vdw} are the van der Waals radii of the atoms, indicates the regions have the ability to intermolecular interactions[19]. The extended form of three-dimensional close contact in a crystal structure gives supramolecular structure.

Theoretical manipulation of the intermolecular interaction of molecular crystals has been accounted by the Hirshfeld surface analysis. It is a powerful technique for determining the degree of atomic or residual contacts within a molecular crystal. We have inspected the

asymmetric unit to examine the Hirshfeld surfaces, which comprise dnorm,[20] shape index, and curvedness (**Figure S4**). In 1 the interactions between O···H atoms are the leading connections.

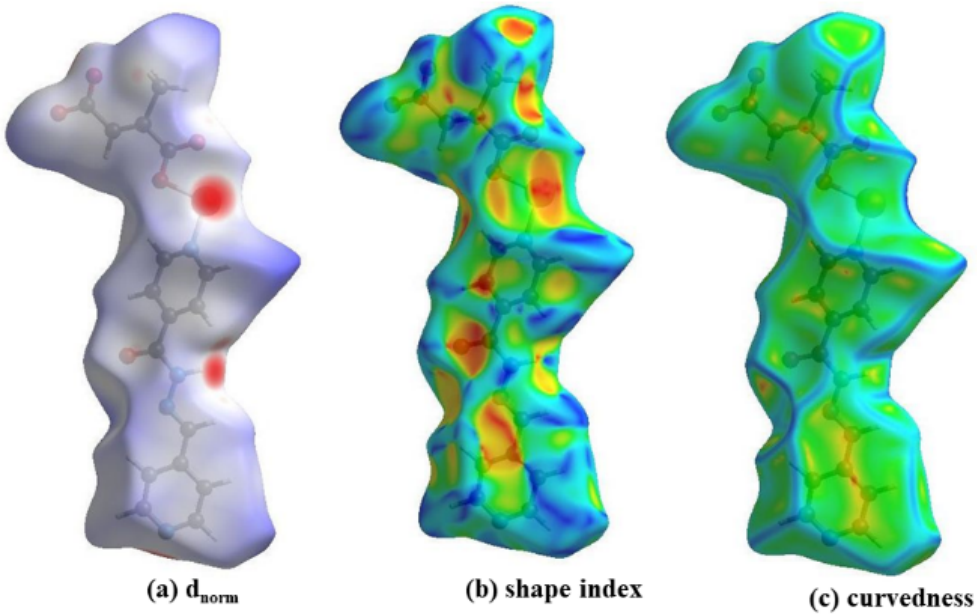

Figure S4. Hirshfeld surfaces mapped over (a) dnorm (b) shape index and (c) curvedness for **1**.

The de and di parameters, which explain the percentage dominance of a specific interaction in creating the supramolecular architecture, are used to construct the 2D fingerprint plots.[21]Using the software Crystal Explorer,[22] the HS is mapped with various attributes and 2D fingerprint plots are produced.

In the presentation of dnorm the colour codes - red, white, and blue patches are used to segregate between distances that are closer, equal, or farther away from van der Waals radii. As a distinctive representative of molecular surfaces, curvature is quantified using curvedness parameters and shape index to add further chemical context to crystal packing. The shape

index displays the molecular surface contacts as corresponding hollows (red) and bumps (blue), whereas the curvedness plot is predominantly made up of sizable green patches, with comparatively flat sections being separated by dark blue lines. Dark-blue edges in both the form index and the curvedness indicate a zone with a higher degree of curvature.

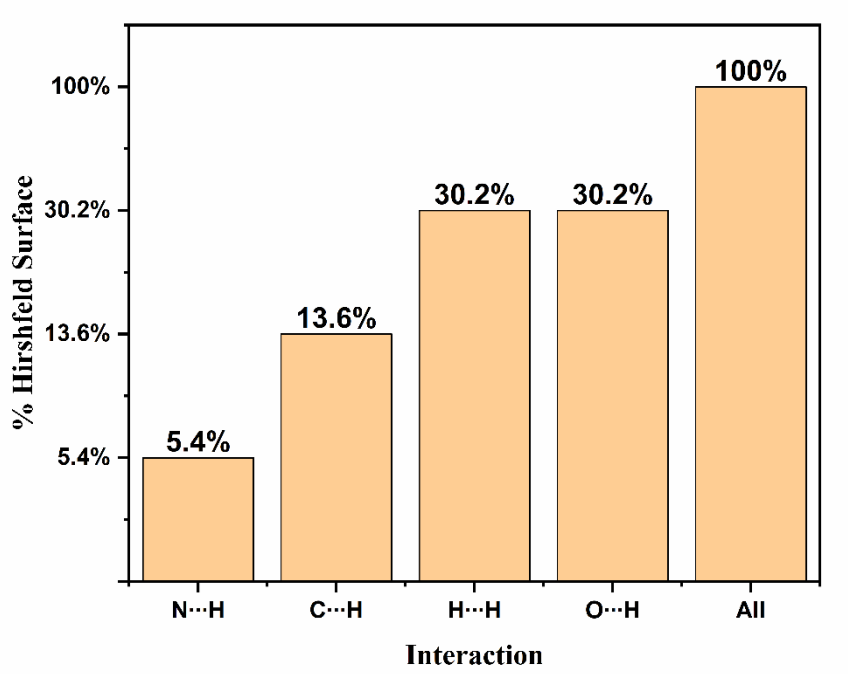

Figure S5: Hirshfeld surface area relative contributions from different intermolecular interactions (O, H, C and N) in **1**.

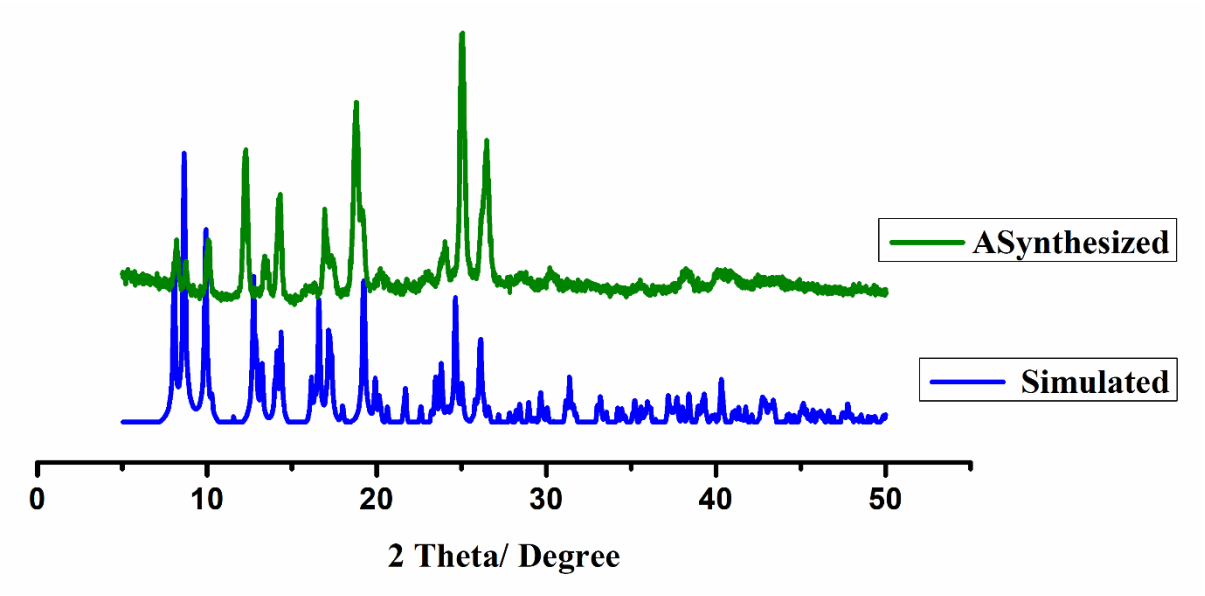

Figure S6. PXRD plot of compound **1.**

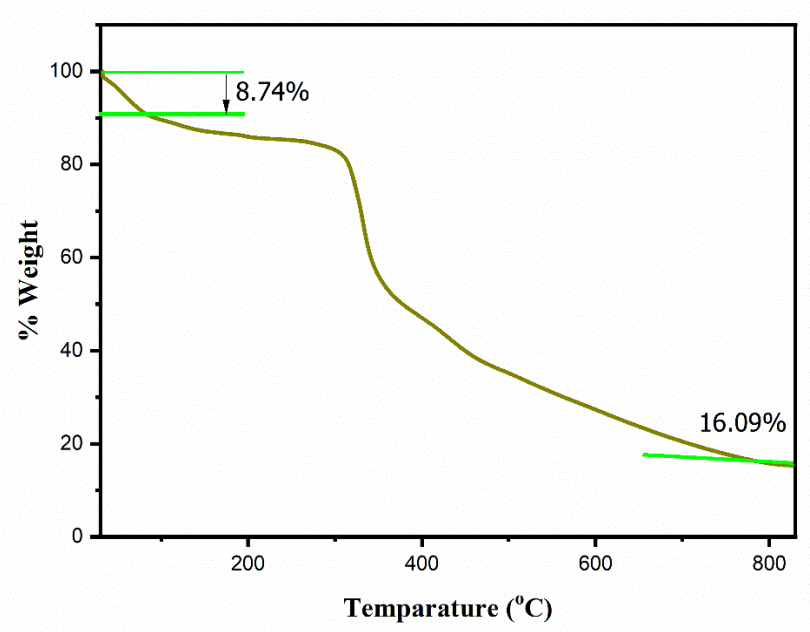

Figure S7. TGA plot of Compound **1.**

Table S1. Selected bond lengths and bond angles in **1.**

Zn(1) - O(3)	2.035(6)	O(4) - C(4)	1.228(11)
Zn(1) - O(4)	2.433(6)	O(5) - C(10)	1.232(15)
Zn(1) - N(4)	2.051(7)	N(1) - C(14)	1.323(13)
Zn(1) - N(1)a	2.067(7)	N(1) - C(16)	1.297(12)
Zn(1) - O(1)c	2.349(9)	N(2) - N(3)	1.358(12)
Zn(1) - O(2)c	2.039(9)	N(2) - C(11)	1.272(12)
O(1) - C(1)	1.215(17)	N(3) - C(10)	1.345(13)
O(2) - C(1)	1.208(16)	N(4) - Zn(1) - N(1)a	101.1(3)
O(3) - C(4)	1.273(11)	N(4) - Zn(1) - O(1)c	91.7(3)
O(3) - Zn(1) - O(4)	57.3(2)	O(3) - Zn(1) - N(1)a	106.8(3)
O(3) - Zn(1) - N(4)	96.8(3)	O(3) - Zn(1) - O(1)c	94.2(3)
N(1)a - Zn(1) - O(1)c	153.7(3)	O(3) - Zn(1) - O(2)c	143.1(3)
C(1) - O(1) - Zn(1)b	83.5(7)	O(3) - Zn(1) - C(1)c	119.6(3)
N(4) - Zn(1) - O(2)c	105.5(3)	O(4) - Zn(1) - N(4)	153.9(2)
O(1)c - Zn(1) - C(1)c	28.6(4)	O(4) - Zn(1) - N(1)a	90.5(2)
O(2)c - Zn(1) - C(1)c	28.3(4)	O(4) - Zn(1) - O(1)c	87.7(3)
N(4) - Zn(1) - C(1)c	100.4(3)	O(4) - Zn(1) - O(2)c	95.9(3)
N(1)a - Zn(1) - O(2)c	97.3(3)	O(4) - Zn(1) - C(1)c	91.5(3)
N(1)a - Zn(1) - C(1)c	125.4(4)	O(1)c - Zn(1) - O(2)c	56.9(4)

a = -1+x,1/2-y,-1/2+z, b = x,3/2-y,-1/2+z, c = x,3/2-y,1/2+z, d= 1+x,1/2-y,1/2+z

Reference:

1. M. J. Frisch, G. W. Trucks, H. B. Schlegel, G. E. Scuseria, M. A. Robb, J. R. Cheeseman, G. Scalmani, V. Barone, B. Mennucci, G. A. Petersson, H. Nakatsuji, M. Caricato, X. Li, H. P. Hratchian, A. F. Izmaylov, J. Bloino, G. Zheng, J. L. Sonnenberg, M. Hada, M. Ehara, K. Toyota, R. Fukuda, J. Hasegawa, M. Ishida, T. Nakajima, Y. Honda, O. Kitao, H. Nakai, T. Vreven, J. A. Montgomery Jr., J. E. Peralta, F. Ogliaro, M. Bearpark, J. J. Heyd, E. Brothers, K. N. Kudin, V. N. Staroverov, R. Kobayashi, J. Normand, K. Raghavachari, A. Rendell, J. C. Burant, S. S. Iyengar, J. Tomasi, M. Cossi, N. Rega, J. M. Millam, M. Klene, J. E. Knox, J. B. Cross, V. Bakken, C. Adamo, J. Jaramillo, R. Gomperts, R. E. Stratmann, O. Yazyev, A. J. Austin, R. Cammi, C. Pomelli, J. W. Ochterski, R. L. Martin, K. Morokuma, V. G. Zakrzewski, G. A. Voth, P. Salvador, J. J. Dannenberg, S. Dapprich, A. D. Daniels, O. Farkas, J. B. Foresman, J. V. Ortiz, J. Cioslowski and D. J. Fox, Gaussian 09, Revision D.01, Gaussian Inc., Wallingford, CT, 2009.
2. A. D. Becke, Density-functional thermochemistry. III. The role of exact exchange, *J. Chem. Phys*., 1993, **98**, 5648–5652.
3. W.R. Wadt and P.J. Hay, *J. Chem. Phys*., 1985, **82**, 299-310.
4. N. M. O'Boyle, A. L. Tenderholt and K. M. Langner, *J. Comput. Chem*., 2008, **29**, 839–845.
5. G. M. Sheldrick, SHELXL 2014, SHELXL-2016/6 and SHELXL-2017/1, Program for Crystal Structure Solution, University of Göttingen, 2014, 2016, 2017.
6. SMART and SAINT; Bruker AXS Inc.: Madison, WI, 1998.
7. Bruker (2001). SADABS. Bruker AXS Inc., Madison, Wisconsin, USA.
8. V. A. Blatov, A. P.Shevchenko and D. M. Proserpio, *Cryst. Growth Des.,* 2014, **14**, 3576–3586.

9. M. O' Keeffe, M. A. Peskov, S. J. Ramsden and O. M. Yaghi, *Acc. Chem. Res.,*2008, **41**, 1782-1789.

10. E. V. Alexandrov, V. A. Blatov, A. V. Kochetkov and D. M. Proserpio, *CrystEngComm.,* 2011, **13**, 3947-3958.

11. T. C. Nicholas, E. V. Alexandrov, V. A. Blatov, A. P. Shevchenko, D. M. Proserpio, A. L. Goodwin and V. L. Deringer, *Chem. Mater.*, 2021, **33**, 8289-8300.

12. E. V. Alexandrov, A. P.Shevchenko and V. A. Blatov, *Cryst. Growth Des.*, 2019, **19**, 2604-2614.

13. F.L. Hirshfeld, *Theor. Chim. Acta*, 1977, **44**, 129-138.

14. A. L. Rohl, M. Moret, W. Kaminsky, K. Claborn, J. J. McKinnon and B. Kahr, *Cryst. Growth Des***.**, 2008, **8**, 4517-4525.

15. A. Parkin, G. Barr, W. Dong, C.J. Gilmore, D. Jayatilaka, J. J. McKinnon, M. A. Spackman and C. C. Wilson, *Cryst. Eng. Comm*., 2007, **9**, 648-652.

16. S. K. Wolff, D. J. Grimwood, J. J. McKinnon, D. Jayatilaka and M. A. Spackman, Crystal Explorer, 2007, **2**.

17. V. Stavila, A. A. Talin and M. D. Allendorf, *Chem. Soc. Rev*., 2014, **43**, 5994-6011.

18. J. Zhang, Y. Huang, D. Yue, Y. Cui, Y. Yang and G. Qian, *J. Mater. Chem*., 2018, **6**, 5174-5180.

19. P. R. Spackman, M. J. Turner, J. J. McKinnon, S. K. Wolff, D. J. Grimwood, D. Jayatilaka and M. A. Spackman, *J. Appl. Cryst*., 2021, **54**, 1006-1011.

20. A. Dey, S. Middya, R. Jana, M. Das, J. Datta, A. Layek, P. P. Ray, *J. Mater. Sci. Mater. Electron.,* 2016, **27**, 6325–6335.

21. M. A. Spackman and J. J. McKinnon, *CrystEngComm.*, 2002, **4**, 378–392.

22. P. R. Spackman, M. J. Turner, J. J. McKinnon, S. K. Wolff, D. J. Grimwood, D. Jayatilaka and M. A. Spackman, *J. Appl. Cryst.,* 2021, **54**, 1006-1011.